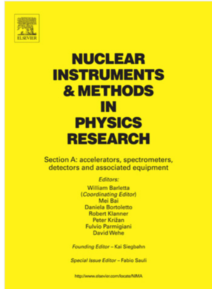

Current-voltage characteristics of silicon PIN diodes irradiated in KAMINI nuclear reactor

Manoj Kumar Parida, S. Tripura Sundari, V. Sathiamoorthy, S. Sivakumar

PII: S0168-9002(18)30846-5
DOI: https://doi.org/10.1016/j.nima.2018.07.014
Reference: NIMA 60960

To appear in: *Nuclear Inst. and Methods in Physics Research, A*

Received date : 26 February 2018
Revised date : 27 June 2018
Accepted date : 6 July 2018

Please cite this article as: M.K. Parida, S.T. Sundari, V. Sathiamoorthy, S. Sivakumar, Current-voltage characteristics of silicon PIN diodes irradiated in KAMINI nuclear reactor, *Nuclear Inst. and Methods in Physics Research, A* (2018), https://doi.org/10.1016/j.nima.2018.07.014

Current-Voltage characteristics of silicon PIN diodes irradiated in KAMINI nuclear reactor

Manoj Kumar Parida[1], S. Tripura Sundari[1]*, V. Sathiamoorthy[2] and S. Sivakumar[2]
[1]Surface and Nanoscience Division, Materials Science Group,
[2]Technical Services Division, Reactors Facilities Group
Indira Gandhi Centre for Atomic Research,
HBNI, Kalpakkam 603102, India

Abstract

The present study reports on the investigation of current voltage (I-V) characteristics of commercial planar Si-PIN diodes, irradiated in a typical thermal nuclear reactor – KAMINI for neutron fluences ranging from $1x10^{14}$ to $1x10^{16}$ n/cm^2. The I-V Characteristics of the virgin and neutron irradiated Si-PIN diodes are measured in ambient environment for the forward and reverse biased conditions. In the forward bias condition, one of the consequences of increasing the neutron irradiation fluence is the increase in knee voltage from ~ 0.5 V for virgin diode to 37.4 V for neutron irradiated diode with fluence $1x10^{16}$ n/cm^2. Further analysis of forward characteristics, revealed increase in ideality factor from a typical value of ~2 for virgin diode to an anomalous value of ~496 for the highest irradiated diode specimen. This increase is attributed to the increasing neutron damage that the diodes undergo upon irradiation. Moreover, in the reverse biased condition, the reverse leakage current increased by four orders magnitude from 10^{-9} to 10^{-5} ampere. A qualitative analysis of the forward and reverse I-V characteristics, showed that the diodes change from a rectifying to ohmic behaviour with increase in fluence and this was inferred from the decrease in 'gap' between the forward and reverse currents in the low voltage regions. Quantitatively, the rectification ratio - ratio of the forward to reverse currents - was calculated to be 10^8 and 84 for the virgin and $1x10^{16}$n/cm^2 irradiated specimens, respectively. The damage constant evaluated from the reverse bias I-V measurements conditions was found to be 1.7683 x 10^{-18} A/cm.

Keywords - Si PIN diode, neutron damage, ideality factor, rectification ratio, electrical characterization

*Corresponding author: sundari@igcar.gov.in

Introduction

In recent years, semiconductor devices have found significant applications for high intensity radiation monitoring in research reactors, solar panels in outer space, lasers in military operations and in high energy physics as particle detectors [1,2]. Among the most widely used semiconductor devices, silicon (Si) PIN diodes have been employed for neutron dosimetry in radiation environment owing to their insensitivity to micro-phonics and amenability to miniaturization [3]. Other distinct inherent advantages of these diodes are fast signal response, good intrinsic detection efficiency, low voltage operation and better energy resolution in terms of pulse height spectra [4]. Moreover, standardization of planar technology process with respect to Si PIN diodes has led to the exploration of a choice of geometries and sizes for optimization of sensitivity of the diode for neutron dose measurement [3]. However, the performances of these devices are susceptible to radiation damage especially from neutrons [5]. It is therefore imperative to study their electrical characteristics from current voltage (I-V) measurements to understand their behaviour in the presence of neutron field. The effects of neutron irradiation on semiconductor Si PIN diodes have been studied in the context of LHC (Large Hardon Collider) too [6].

Several extensive studies on the effect of neutron irradiation on the electrical characteristics have also been conducted as part of ROSE (R&D for Silicon for future Experiments) project [7]. Beattie et al. reported increase in forward voltage of the PIN diode from 10 V to 100 V with increasing neutron fluence [8], when irradiated with neutrons of 1 MeV energy. A similar investigation on I-V characteristics of irradiated silicon detectors performed by Bosetti et al. [9] also, reports the change in the reverse and forward characteristics of diode in terms of rectification ratio, which changes drastically after critical fluence of irradiation. McPherson et al. [10] investigated the electrical characteristics of silicon PIN diodes subjected to 1 MeV neutrons, both prior to and after irradiation. They concluded that the radiation damage occurs only upto certain fluences and beyond that limit, the material becomes resistant to further damage. Additionally, commercial PIN diodes were characterized for their utilization as radiation monitors in LHC to cover 1 MeV equivalent neutrons by Ravotti et al. [11]. They also reported the shifting of the forward characteristics to higher voltages with increase in fluence. However, they obtained a ‘thyristor’ like behaviour for fluences more than $3x10^{13}$ n/cm^2.

Irradiation studies conducted on silicon detectors by Edwards et al. [5] indicate increase in the reverse leakage current of diode after exposure to neutrons. The increase in reverse leakage current is due to the formation of energy levels within the energy band gap [12], which aids in the thermal transition of carriers across the band gap. The I-V characteristics of non silicon based materials like GaAs and GaN exposed to thermal neutron irradiation for fluences upto $3x10^{14}$ n/cm^2 have been studied by Fauzi et al. [13]. They concluded that the performance of diode degraded owing to the displacement damage due to neutrons and gamma ionization. Another neutron irradiation studies on similar GaN materials at higher fluence of 10^{16} n/cm^2 have also been reported by P.Mulligan et al. [14]. They report that the devices showed insignificant change at higher neutron fluence of 10^{15}n/cm^2.

The above experiments have been conducted in controlled environments with respect to energy of the neutrons. There are not many studies on the electrical characterization of PIN diodes when subjected to typical reactor operation conditions also. Hasegawa et al. [15]. reported measurement of I-V characteristics of silicon junction detectors under typical reactor operation conditions. The fluences in their study, however, were limited to $1x10^{14}$ n/cm^2. The evaluated damage constant from their reverse current measurement was typically ~$6.6x10^{-17}$ A/cm, which was two orders lesser than the other neutron irradiation experiments. However, no analysis was carried out to study the variation of the associated diode parameters such as rectification ratio and ideality factor in particular, as a function of neutron fluence, in reactor field conditions. It is therefore worthwhile and essential to examine the electrical behaviour of the Si PIN diodes in particular in real nuclear reactor field conditions so as to study their feasibility of employment in harsh radiation conditions. In the present work, a detailed evolution of forward and reverse I-V electrical characteristics have been investigated on silicon PIN diodes, irradiated in typical thermal research nuclear reactor - KAMINI, for neutron fluences varying from $1x10^{14}$ to $1x10^{16}$ n/cm^2.

Experimental

The experiments were conducted on commercial Si PIN diodes which were procured from M/s Bharat Electronics Limited with the following characteristics. The diode had an active area of 25 mm^2 and surrounded by a guard ring, which not only reduced the reverse leakage current, but also enabled the diode to be operated at higher voltages in reverse bias condition without electrical breakdown [16]. The dark reverse leakage current of diodes were < 10nA/cm^2 and having a maximum operating reverse bias voltage ~ 100V. The window material was made of SiO_2 which is 0.5 μm thick and diodes had an operating temperature ranging from -65 °C to 125 °C.

The neutron irradiations were carried out using a pneumatic fast transfer system in the thermal research nuclear reactor – KAMINI [17], which is a reactor meant for irradiation experiments. The PIN diode specimens were packed in a polythene vial and transferred to the reactor core with a pneumatic fast transfer mechanism. The neutron flux and spectrum at irradiation location have been experimentally measured by the method of foil activation and is shown in figure 7 of ref. [18]. The corresponding neutron fluxes for various energy intervals are summarized in Table 1. The total neutron flux at the irradiation location was 6.01×10^{11} n/cm^2·s, when the reactor power is 20 kW. The irradiation times were so chosen so as to result in neutron fluences 'ϕ' ranging from 1×10^{14} to 1×10^{16} n/cm^2. The ambient temperature at the irradiation location was 300 K. Immediately after the specimens were extricated from the reactor, they had an activity in excess of 10 mR/h, which eventually was below 0.1 mR/h after about 4 hours. This activity was considered fit for handling the specimen and performing electrical measurements. It is to be noted that the diodes were also subjected to gamma dose rate (approx 3.14×10^4 Gy/h). However, the contribution by gamma rays is neglected as the damage caused by it is orders of magnitude lesser than that caused by neutrons [19, 20].

For performing electrical measurements in forward and reverse bias conditions, the diodes were mounted in a Faraday chamber made of Aluminum metal. This chamber was specially designed to shield the diodes from external electromagnetic interference, apart from providing a light free dark environment. The measurements were carried out using Keysight B2912A current source meter. The measurement data were recorded in the PC through the universal serial bus (USB) port. The I-V characteristics in the forward and reverse bias conditions were measured for all the diodes prior to irradiation. For the forward bias condition, the measurements were carried out till 0.8V with a step size of 50 mV, while for the reverse bias conditions, the measurements were carried out from 0 V till 100 V, incrementing at the rate of 1 V. From literature [8], it is known that the forward knee voltage is increased upon irradiation. Therefore, for the measurements of forward currents in irradiated specimens, the upper limit on forward voltage was set at a value where a sharp increase in current was obtained. However, for the reverse bias conditions, the upper voltage (till 100 V) was kept the same as that in the virgin case. In order to estimate the depletion width of Si PIN diode, a reverse C-V measurement was performed using Agilent precision LCR meter (model E4980 A) from 0 V to 100V at constant frequency of 1 MHz.

Results and Discussion

a) Forward Current Analysis

1. Forward I-V characteristics of virgin PIN diode

Figures 1(a) and 1(b) show the response of the forward current (I_f) of virgin PIN diode as a function of forward voltage (V_f) till 0.8V, in the linear and log-log scale, respectively. The forward I-V characteristics show normal rectification behaviour with a sharp increase in I_f close to a knee voltage (V_{knee}) of ~ 0.5 V.

In general, for an ideal PIN diode [21], the forward current voltage (I_f -V_f) relation is given by the equation (1).

$$I_f = I_0 \exp(\beta V_f) + I_{re} \exp(\beta V_f/2) \quad \text{..................(1)}$$

where I_0 and I_{re} are the diffusion and recombination saturation currents, respectively and $\beta = q/\eta kT$, where q is the electronic charge, k is the Boltzmann constant, η is the ideality factor and T is the temperature.

From a linear fitting of I_f vs V_f to Eq. (1) for low and high voltage regions on the semilog scale, the saturation current (I_s) and ideality factor (η), were evaluated from the intercepts and slopes, respectively. A point to note is that the knee voltage 'V_{knee}' is taken as a voltage, above (below) which the total diode current is driven by diffusion (recombination) mechanism. Figure 2 shows the fitting of Eq. (1) for the virgin diode in the recombination and diffusion regions, which yields η =2.1 and I_s = 58.3pA for the low voltage range, while for high voltage range, η= 2.4 and I_s=185 nA. The ideality factor, in general is ~ 1.2 -1.3 and ~2-3 for silicon and GaAs, respectively [22]. For ideal p-n junctions devoid of any defects, the ideality factor is described by Sah–Noyce–Shockley theory [23], which yields η =1 at low voltage range and η=2 at high voltage ranges. Although the experimental ideality factor for the virgin PIN diode indicates a small deviation from the theoretical value ~1(2) for low (high) voltage, the diode is still a good rectifier as seen from the measured reverse leakage current (~ 1.69 nA at 100V) in the reverse bias condition as discussed in later sections. The miniscule magnitude of reverse leakage current clearly indicates that the rectification property of diode is still intact.

2. Forward I-V characteristics of neutron irradiated PIN diodes

Figures 3(a) and 3 (b) show the I_f response of the neutron irradiated Si PIN diodes as a function of V_f, for neutron fluences 'ϕ', ranging from 1×10^{14} n/cm^2 to 1×10^{16} n/cm^2 in the linear scale and log-log scale, respectively.ϕ The plot for the virgin diode specimen is also shown for comparison.

The forward I-V characteristics in these figures definitely show prominent deviations from exponential behaviour of the virgin diode as shown in figures 1(a) and (b). In particular, as ϕ increases, the value of V_{knee} at which the diode reaches limiting current also progressively increases. Therefore, the I-V characteristics of the irradiated diodes could be measured for increased bias voltages without an electrical breakdown of the diodes. The reason for the shift in V_{knee} is due to the formation of traps caused by neutron damage of the Si PIN diode [3]. Higher the neutron fluence, more the neutron damage, thereby leading to shifting V_{knee} to higher voltage levels. As for the analysis, the I-V characteristics are fitted to Eq. (1) for the low and high voltage regions to obtain the ideality factor and saturation currents. A representative fit of the same is shown in figure 4.

The ideality factors and the saturation currents obtained for all the specimens from the fit are shown in figures 5 and 6, respectively. The ideality factor η and the saturation currents consisting of I_o and I_{re}, show distinct increase with increase in ϕ, which indicate considerable deviations from the ideal diode behaviour. The Shockley-Read-Hall (SRH) recombination theory [24] which assumes recombination via isolated point defect levels has been traditionally used to explain the ideality factor (η) in diodes for the diffusion and recombination regions. In the present experiment, η typically changes from ~2 for the virgin diodes to ~ 496 for the highest irradiated fluence. Such large ideality factors have been observed in silicon solar cell devices [25], BN/ZnO hetero structured rectifying diodes, phosphorus doped n-Ge/i-Ge/p-Si hetero-structure diodes too [26]. The increase in ideality factor in the present studies is attributed to the recombination currents being much higher than expected ones [26]. The evolution of increase in η and associated saturation currents with fluence are due to the large defects that are created thereby implying more recombination. Other factors such as tunnelling and metal semiconductor junctions also contribute to high η [26].

Qualitatively, the forward I-V characteristics of all irradiated diodes become more and more shallow with increase in fluence ϕ (figures 3(a) and 3(b)). Moreover, for voltages below the knee voltage of virgin diode, I_f for all the irradiated diodes increases by three orders of magnitude. The large increase in I_f in this region for the lowest irradiated specimen ($1x10^{14}$) is indicative of the damage that the diode undergoes upon irradiation. This increase is attributed to the increased number of electron-hole pairs generated from the generation-recombination centres during the initial stages of irradiation. For higher fluences, the I_f decreases with increase in fluence as shown in figures 3(a) and 3(b). This decrease is due to the formation of traps which are formed by Frenkel defects [3].The traps lead to increased scattering of carriers, resulting in decreased mobility of carriers. Consequently, the lifetime of the charge carriers [3] decreases thereby leading to increased resistance of the material upon irradiation. It is to be noted that even though the diodes were simultaneously exposed to the inevitable gamma dose rate ~ 3.14×10^4 Gy/h, their consequential effect is neglected. This is due to the fact that the gamma ray damage in silicon is almost three orders of magnitude less than that caused by neutrons [19, 20].

In order to further understand the quantitative changes and trends in the evolution of I_f on irradiation, the V_f at which I_f is 17.5 mA, is monitored. This magnitude of I_f is chosen for two reasons. Firstly, the slope of I_f vs V_f is very large at I_f =17.5mA and does not change appreciably with further increase in V_f. Secondly, the current was limited by heating effects to avoid damage to the junction of the diode. The V_f corresponding to 17.5 mA is taken as knee voltage and is plotted in Figure 7 as a function of neutron fluence on a linear scale. It is clear from the graph that, the increase in V_{knee} is maximum in the initial stages of irradiation. The extent of increase in magnitude of V_{knee} with neutron fluence has also been reported in literature by Swartz et al. [27]. With the increase in neutron fluence, trap density is known to increase, which leads to the recombination of generated carriers, thereby decreasing the concentration of the intrinsic charge carriers. Consequently, there is a degradation of carrier lifetime and an increased resistivity upon irradiation. Incidentally, as seen from the fit shown in figure 7, the V_{knee} rises rapidly for low fluences and nearly saturates at a value 36.3 V for a fluence of $5x10^{15}$ n/cm^2. Such saturation behaviour is not reported in ref. [10], probably due to the fact that the I_f

was measured only till ~10-12 volts. The behaviour observed in the present study is almost similar to that reported in Swartz et al. [27] and indicates that there is little change in damage beyond a fluence of $4x10^{15}$ n/cm^2.This ‘flattening off’ is construed to be a consequence of the occupation of displaced atoms and impurities by the Frenkel pairs that have been created by the irradiation, thereby resulting in the material becoming radiation hard or radiation resistant.

b) Reverse current analysis

The I-V characteristics in the reverse bias conditions for the virgin diode along with neutron irradiated diodes are shown in figures 8 and 9 in linear and semilog scale, respectively. The measurements were performed up to a maximum reverse bias voltage ‘V_r’ of 100 V i.e., the limit to which the diodes can be operated in reverse biased condition. Since the interest in the present studies is on the change in characteristics upon neutron irradiation, the I_r-V_r profile of the virgin diode is taken as reference. The reverse leakage current (I_r) due to minority carriers is typically in the nanoampere (10^{-9}A) range for the virgin diode. Apart from the minority carrier contributing to I_r, its magnitude also depends on the active volume of the diode, which in turn is determined by the depletion thickness and lateral extension [28].

As for the neutron irradiated diodes, I_r increases by four orders of magnitude for the diode with lowest irradiated fluence of $1x10^{14}$ n/cm^2. The large change in I_r upon neutron irradiation is due to the fact that a large number of Frenkel pairs are created and unoccupied. Moreover, defect states are introduced upon neutron irradiation and they act as generation-recombination (g-r) centres [10]. These provide e-h pairs that are drawn by the applied reverse field contributing to the increased I_r [29]. It is pointed out that increase in I_r due to the minority charge carriers is a consequence of defects induced by the irradiated neutrons both at the surface and in the bulk of the diode. The increase in I_r is gradual, reaching a maximum value of ~ $5.7x10^{-4}$ A, for the diode irradiated to a fluence of $1x10^{16}$ n/cm^2.

The behaviour of I_r at full depletion voltage which is ~ 100V, in the present experiment is shown in figure 10 as a function of ϕ. This behaviour is comparable to that reported by S.Moloi et al. [30] but does not follow a linear behaviour as reported by Hasegowa et al. [15] and Lemeilleur et al. [29]. Incidentally, a plot of I_r for lower V_r (20V), shows the same trend as V_r of 100V. The behaviour shown in figure 10 implies that change in minority carriers is very large for the lowest fluence and thereafter the change is minimal. The curve tends to flatten indicating that the material is already radiation hard [30].

A qualitative behaviour of the effect of exposure of the diodes to neutrons can be inferred from the gap between the I_f and I_r for both virgin and irradiated diodes. The progressive convergence of 'gap' between the forward and reverse profiles (I_r-I_f) with increase in ϕ is shown in figures 11 (a-c) for a few representative specimens, namely virgin, $1x10^{14}$ n/cm^2 and $5x10^{15}$ n/cm^2 . The progressive decrease in the gap shown in figures 11, is indicative of the change in behaviour from a diode like to ohmic behaviour and compares well with the reported behaviour [30]. The forward and reverse currents are almost equal and vary linearly with applied voltage for high fluences.

The variations in the I-V characteristics are readily brought out by 'rate of change' in the V_{knee} and reverse current I_r obtained from figures 7 and 10, respectively. These rates of change are shown in log-log scale. The reference current and voltage for forward and reverse bias measurements were taken to be 17.5 mA and 100 V, respectively. For the evaluation of slope of V_{knee} with fluence, the data was limited between virgin to $1x10^{15}$ n/cm^2, as beyond this fluence, the V_{knee} saturates. The 'rate of change' of V_{knee} and I_r with fluence are 0.6 and 0.7 respectively, as shown in figures 12 and 13, respectively. The magnitudes of the slopes in the present experiment are nearly comparable and differ from that reported by Moloi et al. [30], where the slope of the reverse bias is reported to be twice that in the forward bias case. The difference in the slopes from ref. [30] is owing to the fact that in the present work the slopes were estimated till low neutron fluence as saturation in V_{knee} was observed at higher fluence.

Damage Constant

The damage constant 'α' or volume reverse leakage current I_r/V_l, in the reverse bias conditions is taken as a measure of the damage caused by irradiation [31] and I_r is used to evaluate the radiation hardness property of the diode [31,32]. The constant 'α' is defined through the relation, $\Delta I=\alpha V_l$, where, ΔI is the difference in the reverse leakage current for the irradiated and virgin diode for the full depletion voltage of 100V and V_l is the volume of the depletion region in the diode. The lateral dimension of the PIN diodes used in the experiments is 5mm x 5mm and the width of the depletion region was computed from a measurement of capacitance in reverse bias conditions(C-V). Figure 14 shows the reverse C-V measurement of virgin diode ($1x10^{16}$ n/cm^2) in which the capacitance (C) decreases with increase in reverse voltage and becomes constant beyond 60 V. The initial decrease in capacitance is attributed to the increase in depletion width of diode with voltage, while the invariance above a certain voltage (~60V) indicates a complete depletion of the diode. The depletion region width estimated from the C-V measurement is ~300µm [33].

The difference in the I_r per unit volume estimated at the reverse bias voltage of 100V for all the five irradiated diodes is shown in figure 15. From a linear fitting of ΔI vs ϕ, the damage constant α is estimated to be 1.7683×10^{-18}(A/cm).The damage constant 'α' in this experiment is lesser compared to that reported in ref. [15]. This is due to use of a wide spectrum of incident neutrons energy rather than a monoenergetic neutron beam.

Rectification ratio (RR)

It is well known that the I-V characteristics, which demonstrate the rectifying behaviour, are crucial for device applications. In the context of diodes, rectification is monitored and quantified in terms of rectifying ratio 'RR', which expresses the ratio of the I_f to the I_r. Mathematically, RR is

$$RR = \frac{I_{fV_{f,max}}}{I_{rV_{f,max}}} \dots\dots\dots\dots\dots\dots (2)$$

In the above expression, $V_{f,max}$ is the maximum forward voltage of the diode which can be applied within the permissible limits of operation and is used as the reference voltage for calculation of the RR. In the present experiment, as seen from figure 3(a), V_{fmax} varies with the neutron irradiation fluence. As seen from the graph (see figure 16), the virgin diode has the highest rectification ratio RR of ~10^8, with the current conduction in one direction only. This high value of RR is owing to the fact that the I_f is in the mA range, while the leakage current in the reverse bias condition is in the nA range. Large RR has also been reported in all printed organic diodes [34] and metal induced lateral crystallization in a-Si: H in solar cell application [35].

In the present experiment, RR decreases drastically to ~ 10^3 and ~84 for diodes exposed to ϕ of $1x10^{14}$ n/cm^2 and $1x10^{16}$ n/cm^2, respectively as shown in figure 16. This decreasing trend is consistent with that observation by Bosetti et al. [9], although the magnitudes vary. The decrease in RR clearly indicates that the neutron irradiated diodes progressively lose their rectifying behaviour with increasing ϕ. The reason for the loss of rectifying behaviour is the decrease (increase) in the concentration of majority (minority) charge carriers. It is well known that irradiation induces defects and leads to loss of crystallinity, thereby resulting in decreased lifetime and mobility [3] .Such defect centres are known to increase the reverse leakage current and consequently resulting in loss of rectification [9].The variation of RR vs ϕ has been studied in literature and a critical fluence was observed [9] in which the RR is equal to zero. However, in the present experiment, it is found that the RR is ~ 84 even for a fluence of $1x10^{16}$ n/cm^2, which is higher than that reported in ref [9].

The quantities, RR and η are inverse to each other and the same is shown in figure 17. A large RR results in nearly ideal diodes where the ideality factor is ~1 in the diffusion region. It is pertinent to note that the ideality factor of an ideal diode is 1(2) in the diffusion (recombination) region with the concomitant RR being very large (typically 10^{8} or more). Figure 17 indicates a clear change in the behaviour of the diode from a rectifying one to ohmic one. This is a consequence of deceasing (increasing) forward (reverse) current with increasing fluence. Such a correlation has also been reported for nanocrystalline pn diodes [35].

Conclusion

This paper discusses the effect of neutron irradiation on the current voltage characteristics of silicon PIN diodes in a typical thermal research reactor for fluences ranging from $1x10^{14}$ to $1x10^{16}$ n/cm^2. The measured forward I-V characteristics, is increasingly becoming shallow upon increased irradiation fluence. Moreover, the knee voltage increases from 0.5V for the virgin diode to ~ 36.3 V for diode irradiated to a fluence of ~ $5x10^{15}$ n/cm^2 and thereafter saturates. The shift and increase in knee voltage is attributed to increased trap density [36], which in turn leads to the recombination of the majority carriers, thereby decreasing the concentration of the intrinsic charge carriers. The increase in knee voltage indicates that diodes can be operated at higher voltages [37].The ideality factors extracted from the fit of the forward I-V characteristics to diode equations in the low/high voltage regions varied from a typical value of ~ 2 for the virgin case to ~ 496 for the highest irradiated fluence. The large ideality factors observed in this study are caused by the defects that are created upon irradiation.

With increase in neutron fluence, the reverse leakage currents also increased by almost four orders of magnitude owing to the production of a large number of defect states that act as generation-recombination (g-r) centres upon neutron irradiation. Another important consequence of the increase in fluence of irradiation is the transformation of diode properties from a rectifying to ohmic one, which was inferred from the progressive decrease in gap between the forward and reverse currents. Further, quantitatively, the rectification ratio decreased from 10^8 for virgin diode to 84 for the maximum neutron irradiated fluence of $1x10^{16} n/cm^2$. The damage constant evaluated from the reverse leakage current indicates that the diode hardness property is still in intact after the irradiation. The quantitative behaviour of diodes in terms of rectification ratio shows that its rectification property has been degraded drastically with the increase in neutron fluence.

Acknowledgement

Authors would like to thank Director, IGCAR, Director, MSG for encouragement and support. The authors would also like to acknowledge Dr. S. Dhara Head ,SND for going through the manuscript critically and giving his inputs. One of the authors Manoj Kumar Parida would like to thank DAE for providing SRF fellowship.

References

[1] N.I.C. Omar, N.K.A.M. Rashid, J.A. Karim, J. Abdullah, N.F. Hasbullah, Effects of neutron on reverse bias characteristics of commercially available Si and GaAs diodes, Aust. J. Basic Appl. Sci. 6 (2012) 211–216.

[2] G.Lutz, Semiconductor and electronic devices, Springer, 1999.

[3] I. Anokhin, O. Zinets, A. Rosenfeld, M. Lerch, M. Yudelev, V. Perevertaylo, M. Reinhard, M. Petasecca, Studies of the Characteristics of a Silicon Neutron Sensor, IEEE Trans. Nucl. Sci. 56 (2009) 2290–2293. doi:10.1109/TNS.2009.2024150.

[4] S.J. Bates, D.J. Munday, M.A. Parker, F. Anghinolfi, A. Chilingarov, A. Ciasnohova, M. Glaser, E. Heijne, P. Jarron, F. Lemeilleur, J.C. Santiard, R. Bonino, A.G. Clark, H. Kambara, C. Gössling, B. Lisowski, A. Rolf, S. Pilath, H. Feick, E. Fretwurst, G. Lindström, T. Schulz, R.A. Bardos, G.W. Gorfine, G.F. Moorhead, G.N. Taylor, S.N. Tovey, Recent results of radiation damage studies in silicon, Nucl. Instrum. Methods Phys. Res. Sect. Accel. Spectrometers Detect. Assoc. Equip. 344 (1994) 228–236. doi:10.1016/0168-9002(94)90675-0.

[5] M. Edwards, G. Hall, S. Sotthibandhu, Neutron radiation damage studies of silicon detectors, Nucl. Instrum. Methods Phys. Res. Sect. Accel. Spectrometers Detect. Assoc. Equip. 310 (1991) 283–286. doi:10.1016/0168-9002(91)91044-V.

[6] M. Moll, Development of radiation hard sensors for very high luminosity colliders—CERN-RD50 project, Nucl. Instrum. Methods Phys. Res. Sect. Accel. Spectrometers Detect. Assoc. Equip. 511 (2003) 97–105. doi:10.1016/S0168-9002(03)01772-8.

[7] G. Lindström, M. Ahmed, S. Albergo, P. Allport, D. Anderson, L. Andricek, M.M. Angarano, V. Augelli, N. Bacchetta, P. Bartalini, R. Bates, U. Biggeri, G.M. Bilei, D. Bisello, D. Boemi, E. Borchi, T. Botila, T.J. Brodbeck, M. Bruzzi, T. Budzynski, P. Burger, F. Campabadal, G. Casse, E. Catacchini, A. Chilingarov, P. Ciampolini, V. Cindro, M.J. Costa, D. Creanza, P. Clauws, C. Da Via, G. Davies, W. De Boer, R. Dell'Orso, M. De Palma, B. Dezillie, V. Eremin, O. Evrard, G. Fallica, G. Fanourakis, H. Feick, E. Focardi, L. Fonseca, E. Fretwurst, J. Fuster, K. Gabathuler, M. Glaser, P. Grabiec, E. Grigoriev, G. Hall, M. Hanlon, F. Hauler, S. Heising, A. Holmes-Siedle, R. Horisberger, G. Hughes, M. Huhtinen, I. Ilyashenko, A. Ivanov, B.K. Jones, L.

Jungermann, A. Kaminsky, Z. Kohout, G. Kramberger, M. Kuhnke, S. Kwan, F. Lemeilleur, C. Leroy, M. Letheren, Z. Li, T. Ligonzo, V. Linhart, P. Litovchenko, D. Loukas, M. Lozano, Z. Luczynski, G. Lutz, B. MacEvoy, S. Manolopoulos, A. Markou, C. Martinez, A. Messineo, M. Mikuž, M. Moll, E. Nossarzewska, G. Ottaviani, V. Oshea, G. Parrini, D. Passeri, D. Petre, A. Pickford, I. Pintilie, L. Pintilie, S. Pospisil, R. Potenza, C. Raine, J.M. Rafi, P.N. Ratoff, R.H. Richter, P. Riedler, S. Roe, P. Roy, A. Ruzin, A.I. Ryazanov, A. Santocchia, L. Schiavulli, P. Sicho, I. Siotis, T. Sloan, W. Slysz, K. Smith, M. Solanky, B. Sopko, K. Stolze, B. Sundby Avset, B. Svensson, C. Tivarus, G. Tonelli, A. Tricomi, S. Tzamarias, G. Valvo, A. Vasilescu, A. Vayaki, E. Verbitskaya, P. Verdini, V. Vrba, S. Watts, E.R. Weber, M. Wegrzecki, I. Wegrzecka, P. Weilhammer, R. Wheadon, C. Wilburn, I. Wilhelm, R. Wunstorf, J. Wüstenfeld, J. Wyss, K. Zankel, P. Zabierowski, D. Žontar, Radiation hard silicon detectors—developments by the RD48 (ROSE) collaboration, Nucl. Instrum. Methods Phys. Res. Sect. Accel. Spectrometers Detect. Assoc. Equip. 466 (2001) 308–326. doi:10.1016/S0168-9002(01)00560-5.

[8] L.J. Beattie, A. Chilingarov, T. Sloan, Forward-bias operation of Si detectors:: a way to work in high-radiation environment, Nucl. Instrum. Methods Phys. Res. Sect. Accel. Spectrometers Detect. Assoc. Equip. 439 (2000) 293–302. doi:10.1016/S0168-9002(99)00840-2.

[9] M. Bosetti, N. Croitoru, C. Furetta, C. Leroy, S. Pensotti, P. Rancoita, M. Rattaggi, M. Redaelli, A. Seidman, Study of current-voltage characteristics of irradiated silicon detectors, Nucl. Instrum. Methods Phys. Res. Sect. B Beam Interact. Mater. At. 95 (1995) 219–224. doi:10.1016/0168-583X(94)00439-0.

[10] M. McPherson, B.K. Jones, T. Sloan, Effects of radiation damage in silicon p - i - n photodiodes, Semicond. Sci. Technol. 12 (1997) 1187. doi:10.1088/0268-1242/12/10/003.

[11] F. Ravotti, M. Glaser, M. Moll, F. Saigne, BPW34 Commercial p-i-n Diodes for High-Level 1-MeV Neutron Equivalent Fluence Monitoring, IEEE Trans. Nucl. Sci. 55 (2008) 2133–2140. doi:10.1109/TNS.2008.2000765.

[12] A. Ruzin, Recent results from the RD-48 (ROSE) Collaboration, Nucl. Instrum. Methods Phys. Res. Sect. Accel. Spectrometers Detect. Assoc. Equip. 447 (2000) 116–125. doi:10.1016/S0168-9002(00)00179-0.

[13] D.A. Fauzi, N.K.A.M. Rashid, J.A. Karim, M.R.M. Zin, N.F. Hasbullah, O.A.S. Fareed, Electrical performances of commercial GaN and GaAs based optoelectronics under neutron irradiation, IOP Conf. Ser. Mater. Sci. Eng. 53 (2013) 012029. doi:10.1088/1757-899X/53/1/012029.

[14] P. Mulligan, J. Qiu, J. Wang, L.R. Cao, Study of GaN radiation sensor after in-core neutron irradiation, in: 2013 3rd International Conference on Advancements in Nuclear Instrumentation, Measurement Methods and Their Applications (ANIMMA), 2013: pp. 1–5. doi:10.1109/ANIMMA.2013.6727935.

[15] M. Hasegawa, S. Mori, T. Ohsugi, H. Kojima, A. Taketani, T. Kondo, M. Noguchi, Radiation damage of silicon junction detectors by neutron irradiation, Nucl. Instrum. Methods Phys. Res. Sect. Accel. Spectrometers Detect. Assoc. Equip. 277 (1989) 395–400. doi:10.1016/0168-9002(89)90768-7.

[16] V.Mishra, V.D.Srivastava,S.K.Kataria,Role of guard rings in improving the performance of silicon detectors, Pramana-Journal of Physics. 65 (2005) 259-272.

[17] D.K. Mohapatra, P. Mohanakrishnan, Measurement and prediction of neutron spectra in the Kalpakkam mini reactor (KAMINI), Appl. Radiat. Isot. Data Instrum. Methods Use Agric. Ind. Med. 57 (2002) 25–33.

[18] G.V.S.A. Kumar, S. Sen, E. Radha, J.S.B. Rao, R. Acharya, R. Kumar, C.R. Venkatasubramani, A.V.R. Reddy, M. Joseph, Studies on neutron spectrum characterization for the Pneumatic Fast Transfer System (PFTS) of KAMINI reactor, Appl. Radiat. Isot. 124 (2017) 49–55. doi:10.1016/j.apradiso.2017.03.009.

[19] J.R. Srour, D.M. Long, D.G. Millward, R.L. Fitzwilson and W.L. Chadsey, Radiation damage of silicon junction detectors Enhancement of Electronic Materials, (Noyes Publications), 1984.

[20] J.P. Raymond, E.L. Petersen, Comparison of Neutron, Proton and Gamma Ray Effects in Semiconductor Devices, IEEE Transactions on Nuclear Science. 34 (1987) 1621–1628. doi:10.1109/TNS.1987.4337526.

[21] A. Bar-Lev, Semiconductor and electronic devices, Prentice-Hall, 1993.

[22] V.R.V. Pillai, S.K. Khamari, V.K. Dixit, T. Ganguli, S. Kher, S.M. Oak, Effect of γ-ray irradiation on breakdown voltage, ideality factor, dark current and series resistance of GaAs p–i–n diode, Nucl. Instrum. Methods Phys. Res. Sect. Accel. Spectrometers Detect. Assoc. Equip. 685 (2012) 41–45. doi:10.1016/j.nima.2012.05.062.

[23] C.Sah,R.N. Noyce,W. Shockley, Carrier Generation and Recombination in p-n Junctions and p-n Junction Characteristics. Proceedings of the IRE 45 (1957) 1228-1243. http://dx.doi.org/10.1109/JRPROC.1957.278528

[24] W. Shockley, W.T. Read, Statistics of the Recombinations of Holes and Electrons, Phys. Rev. 87 (1952) 835–842. doi:10.1103/PhysRev.87.835.

[25] O. Breitenstein, P. Altermatt, K. Ramspeck, A. Schenk, The Origin of Ideality Factors N> 2 of Shunts and Surfaces in the Dark I-V Curves of Si Solar Cells, n.d.,21st European Photovoltaic Solar Energy Conference., 2006.

[26] M. Brötzmann, U. Vetter, H. Hofsäss, BN/ZnO heterojunction diodes with apparently giant ideality factors, J. Appl. Phys. 106 (2009) 063704. doi:10.1063/1.3212987.

[27] J.M. Swartz, M.O. Thurston, Analysis of the Effect of Fast-Neutron Bombardment on the Current-Voltage Characteristic of a Conductivity-Modulated p-i-n Diode, J. Appl. Phys. 37 (1966) 745–755. doi:10.1063/1.1708249.

[28] Y. Murakami, T. Shingyouji, Separation and analysis of diffusion and generation components of pn junction leakage current in various silicon wafers, J. Appl. Phys. 75 (1994) 3548–3552. doi:10.1063/1.356091.

[29] F. Lemeilleur, M. Glaser, E.H.M. Heijne, P. Jarron ,E. Occelli, Neutron-induced radiation damage in silicon detectors,IEEE Transactions on Nuclear Science, 39, 1992 551-557.

[30] S.J. Moloi, M. McPherson, The current and capacitance response of radiation-damaged silicon PIN diodes, Phys. B Condens. Matter. 404 (2009) 3922–3929. doi:10.1016/j.physb.2009.07.123.

[31] G. Lindström, M. Moll, E. Fretwurst, Radiation hardness of silicon detectors – a challenge from high-energy physics, Nucl. Instrum. Methods Phys. Res. Sect. Accel. Spectrometers Detect. Assoc. Equip. 426 (1999) 1–15. doi:10.1016/S0168-9002(98)01462-4.

[32] F.Honniger, Radiation Damage in Silicon - Defect Analysis and Detector Properties, Ph.D dissertation submitted in 2007.

[33] V.Mishra, Study of Silicon Detectors, Ph.D dissertation submitted in 2002 , Mumbai University.

[34] S. Ali, J. Bae, C.H. Lee, Organic diode with high rectification ratio made of electrohydrodynamic printed organic layers, Electron. Mater. Lett. 12 (2016) 270–275. doi:10.1007/s13391-015-5202-y.

[35] J.D. Hwang, K.S. Lee, A High Rectification Ratio Nanocrystalline p–n Junction Diode Prepared by Metal-Induced Lateral Crystallization for Solar Cell Applications, J. Electrochem. Soc. 155 (2008) H259–H262. doi:10.1149/1.2840618.

[36] V. Sopko, B. Sopko, D. Chren, J. Dammer, Study of PIN diode energy traps created by neutrons, J. Inst. 8 (2013) C03014. doi:10.1088/1748-0221/8/03/C03014.

[37] A. Chilingarov, T. Sloan, Operation of heavily irradiated silicon detectors under forward bias, Nuclear Instruments and Methods in Physics Research Section A: Accelerators, Spectrometers, Detectors and Associated Equipment. 399 (1997) 35–37. doi:10.1016/S0168-9002(97)00940-6.

Table Captions

Table 1. Neutron spectrum and flux measured at neutron irradiation location.

Figure Captions

Figure 1 Forward I-V Characteristics of virgin diode in (a) linear and (b) log-log scale.

Figure 2 Fitting of diode equation (Eq. 1) for low and high voltage regions for virgin diode, in order to obtain ideality factor (η) and saturation current (I_s) in the respective region.

Figure 3 Forward I-V Characteristics of neutron irradiated diodes in (a) linear and (b) log-log scale.

Figure 4 Fitting of diode equation (Eq.1) to a typical neutron irradiated diode (ϕ=1 x10^{15}n/cm^2) for low and high voltage regions.

Figure 5 Variation of η with neutron fluence ϕ (n/cm^2), obtained from fit to Eq. 1 for low and high voltage ranges (Note: line is guide to the eye).

Figure 6 Variation of saturation current with neutron fluence ϕ (n/cm^2) obtained from fit to Eq.1 for low and high voltage range (Note: line is guide to the eye).

Figure 7 Variation of knee voltage (V_{knee}) with neutron fluence at constant forward current of 17.5 mA.

Figure 8 Reverse I-V characteristics of virgin and neutron irradiated diodes in linear scale.

Figure 9 Reverse I-V characteristics of virgin and neutron irradiated diodes in semi-log scale.

Figure 10 Reverse leakage current at bias voltage of 20V and 100 V as a function of neutron fluence.

Figure 11 Low voltage gap between I_f and I_r for (a) virgin (b) 5x10^{14} n/cm^{2}and (c) 5x10^{15}n/cm^2 showing the progressive decrease in gap between I_f and I_r with increasing fluence.

Figure 12 'Rate of change' of knee voltage at forward current of 17.5mA with neutron fluence in log-log scale.

Figure 13 'Rate of change' of reverse current with neutron fluence in log-log scale.

Figure 14 Reverse capacitance voltage characteristics of virgin diode.

Figure 15 Variation of current density with neutron fluence and slope showing the damage constant 'α'.

Figure 16 Variation of rectification ratio RR of virgin and neutron irradiated diodes as function of neutron fluence ϕ (n/cm^2).

Figure 17 Variation of rectification ratio RR and ideality factor (η) with neutron fluence ϕ (n/cm^2).

Table.1

Neutron Energy Interval	Neutron Flux ($cm^{-2} \cdot s^{-1}$)
0 - 0.56 eV	3.45 $x10^{10}$
0.56 ev – 0.5 MeV	4.30 $x10^{11}$
0.5 MeV- 2 MeV	1.36 $x10^{11}$

Figure 1

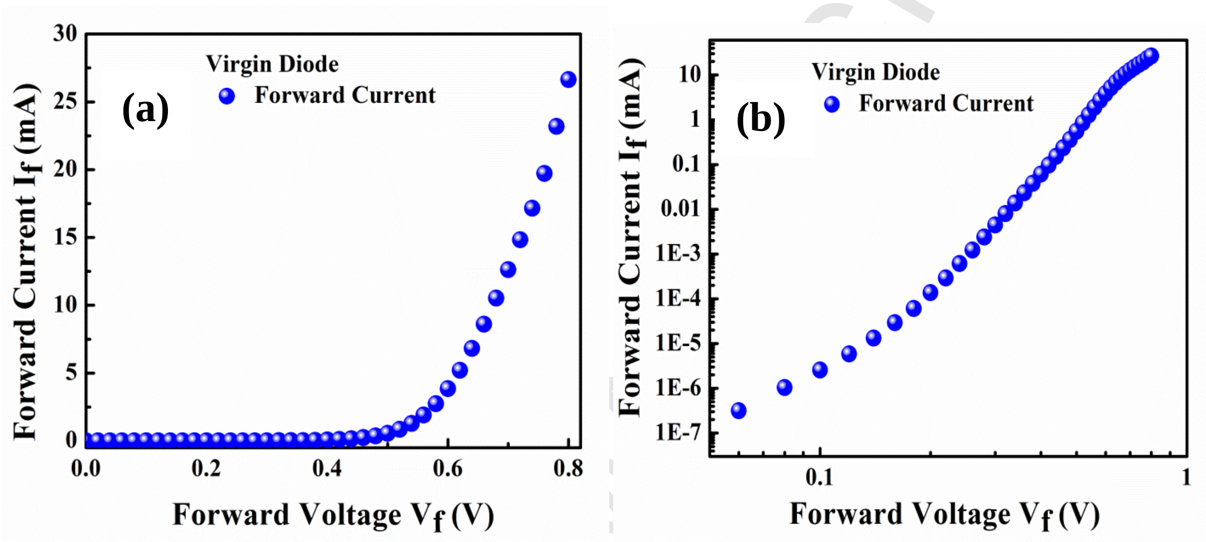
(a)
Virgin Diode
Forward Current
Forward Current I_f (mA)
30
25
20
15
10
5
0
0.0
0.2
0.4
0.6
0.8
Forward Voltage V_f (V)
(b)
Virgin Diode
Forward Current
Forward Current I_f (mA)
10
1
0.1
0.01
1E-3
1E-4
1E-5
1E-6
1E-7
0.1
1
Forward Voltage V_f (V)

Figure 2

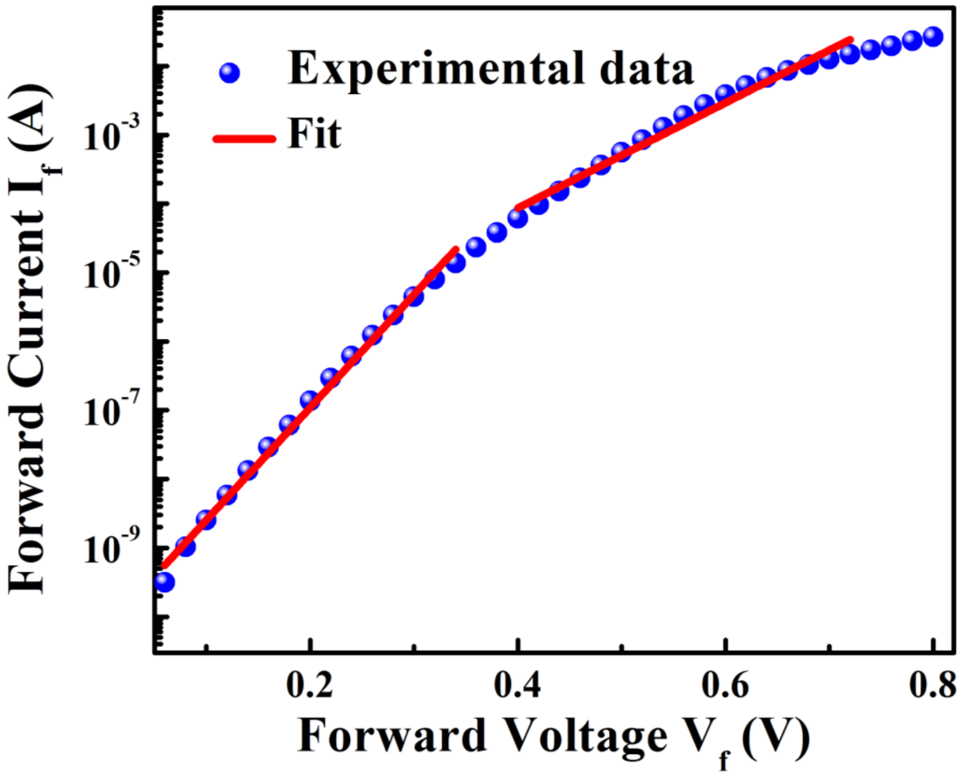
Experimental data
Fit
Forward Current I_f (A)
10^{-3}
10^{-5}
10^{-7}
10^{-9}
0.2
0.4
0.6
0.8
Forward Voltage V_f (V)

Figure 3

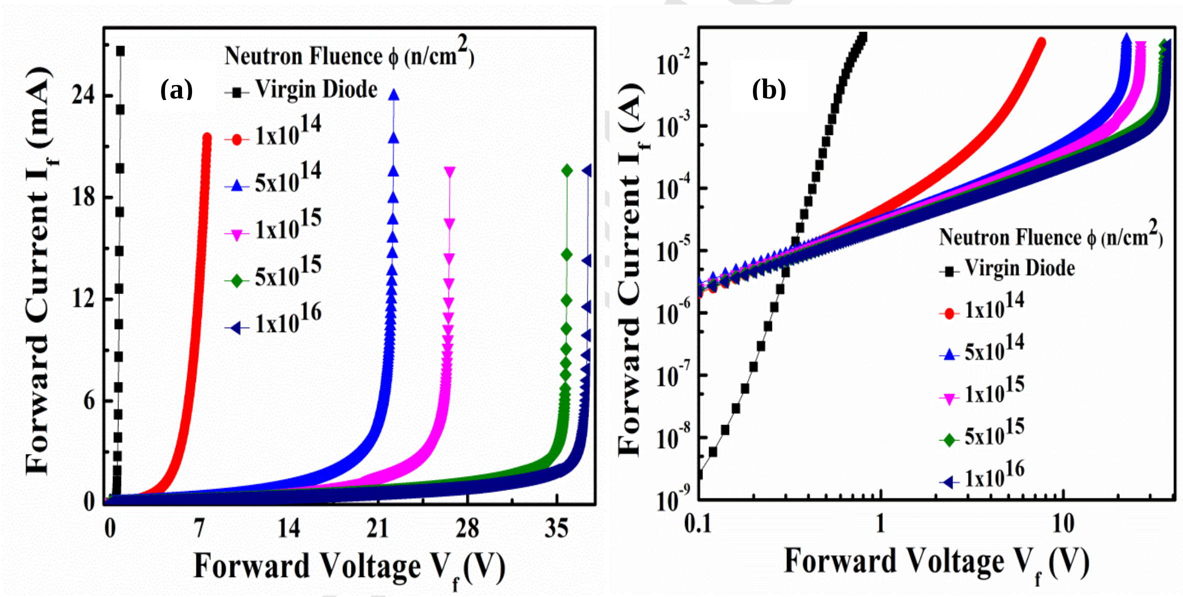
(a)
Neutron Fluence ϕ (n/cm2)
Virgin Diode
1x1014
5x1014
1x1015
5x1015
1x1016
Forward Current If (mA)
Forward Voltage Vf (V)
0
6
12
18
24
0
7
14
21
28
35
(b)
Neutron Fluence ϕ (n/cm2)
Virgin Diode
1x1014
5x1014
1x1015
5x1015
1x1016
Forward Current If (A)
Forward Voltage Vf (V)
10-2
10-3
10-4
10-5
10-6
10-7
10-8
10-9
0.1
1
10

Figure 4

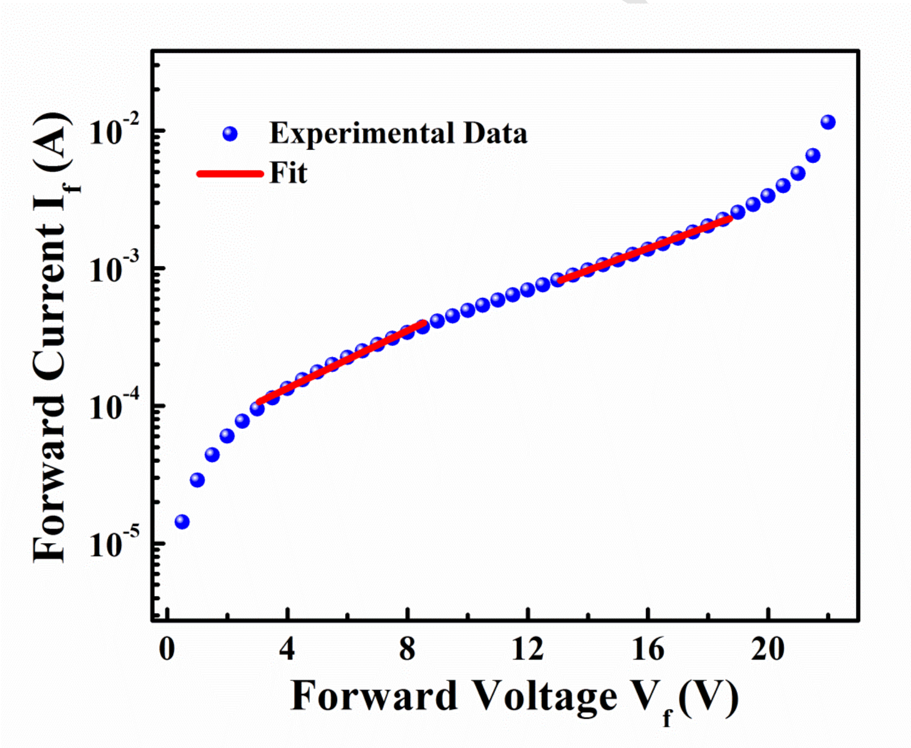
Experimental Data
Fit
Forward Current I$_f$ (A)
10^{-2}
10^{-3}
10^{-4}
10^{-5}
0
4
8
12
16
20
Forward Voltage V$_f$ (V)

Figure 5

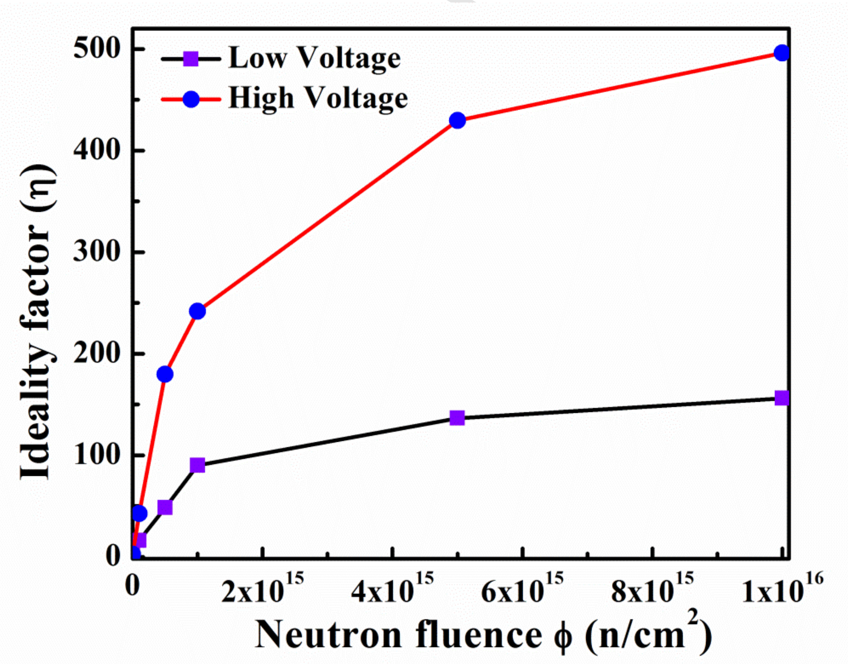
Low Voltage
High Voltage
Ideality factor (η)
Neutron fluence ϕ (n/cm^2)
0
100
200
300
400
500
2x10^15
4x10^15
6x10^15
8x10^15
1x10^16

Figure 6

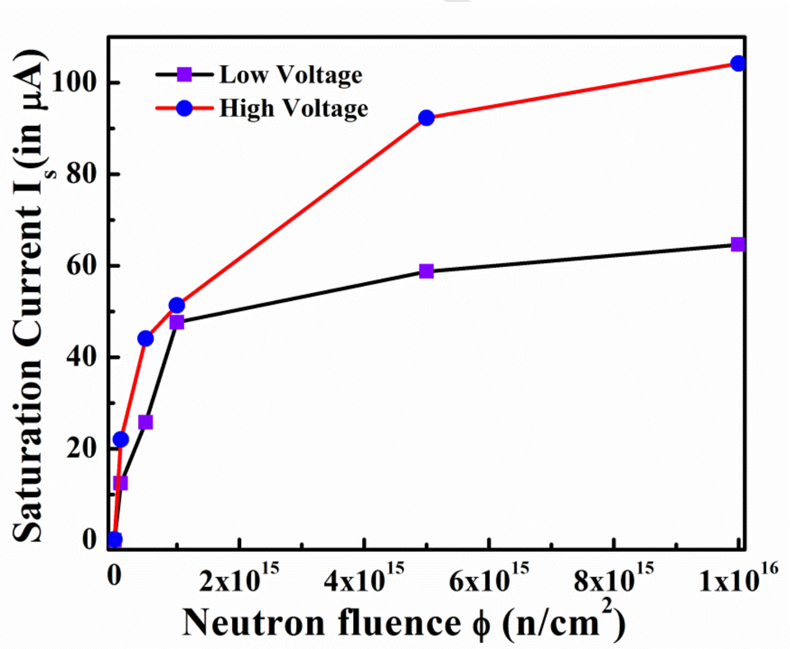
Low Voltage
High Voltage
Saturation Current I_s (in μA)
0
20
40
60
80
100
0
$2x10^{15}$
$4x10^{15}$
$6x10^{15}$
$8x10^{15}$
$1x10^{16}$
Neutron fluence ϕ (n/cm^2)

Figure 7

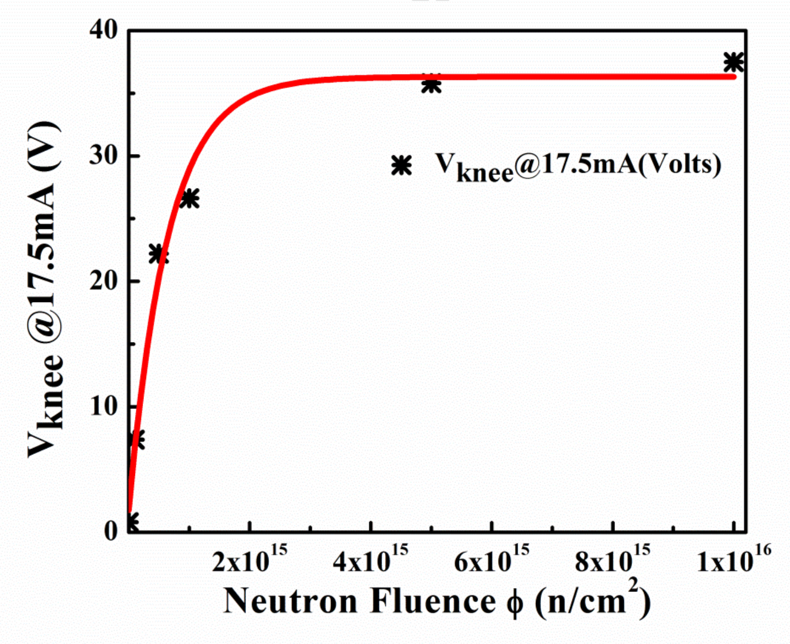

40
30
20
10
0
2x10^15
4x10^15
6x10^15
8x10^15
1x10^16
Neutron Fluence ϕ (n/cm^2)
V_knee @17.5mA (V)
V_knee@17.5mA(Volts)

Figure 8

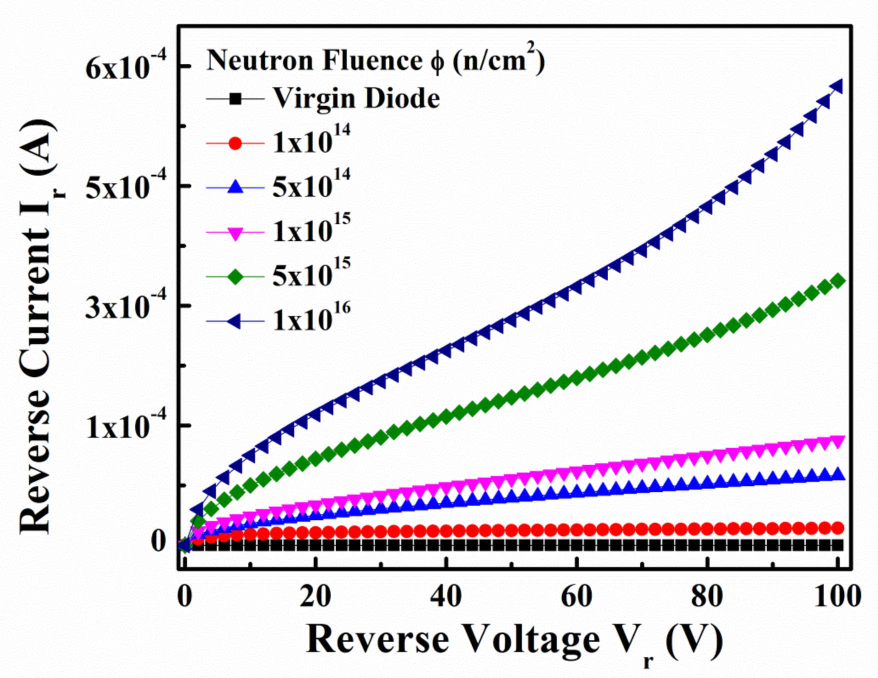

Neutron Fluence ϕ (n/cm^2)
Virgin Diode
1x10^{14}
5x10^{14}
1x10^{15}
5x10^{15}
1x10^{16}
6x10^{-4}
5x10^{-4}
3x10^{-4}
1x10^{-4}
0
Reverse Current I$_r$ (A)
0
20
40
60
80
100
Reverse Voltage V$_r$ (V)

Figure 9

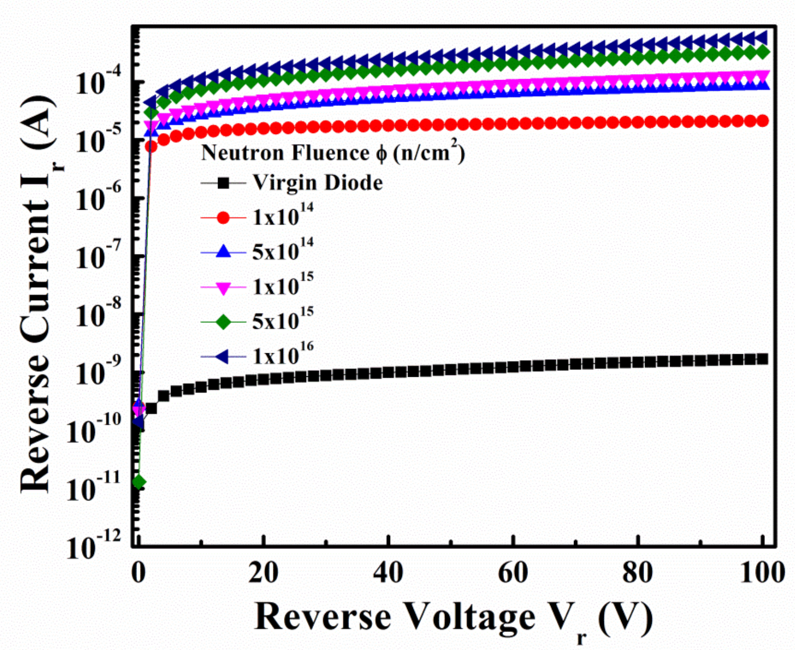

Reverse Current I_r (A)
Reverse Voltage V_r (V)
Neutron Fluence ϕ (n/cm^2)
Virgin Diode
1x10^{14}
5x10^{14}
1x10^{15}
5x10^{15}
1x10^{16}

Figure 10

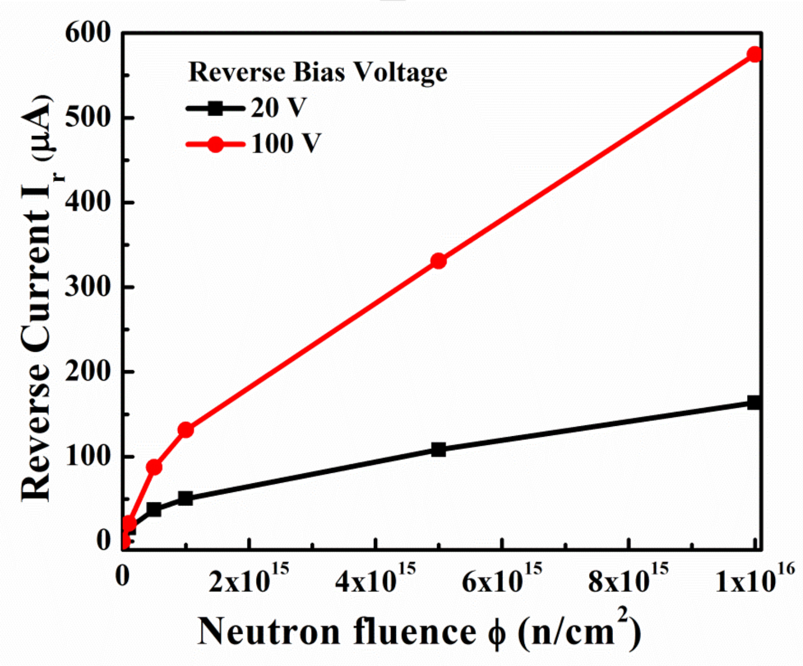

Reverse Bias Voltage
20 V
100 V
Reverse Current I_r (μA)
Neutron fluence ϕ (n/cm^2)
0
100
200
300
400
500
600
$2x10^{15}$
$4x10^{15}$
$6x10^{15}$
$8x10^{15}$
$1x10^{16}$

Figure 11

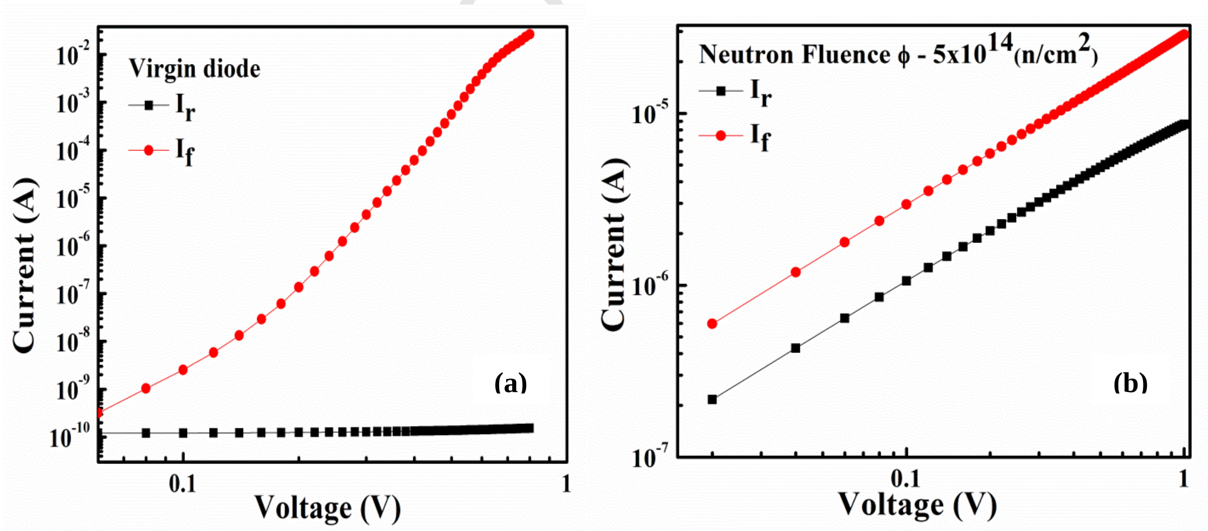

Virgin diode
I_r
I_f
(a)
Current (A)
Voltage (V)
Neutron Fluence ϕ - 5x10[14](n/cm[2])
I_r
I_f
(b)
Current (A)
Voltage (V)

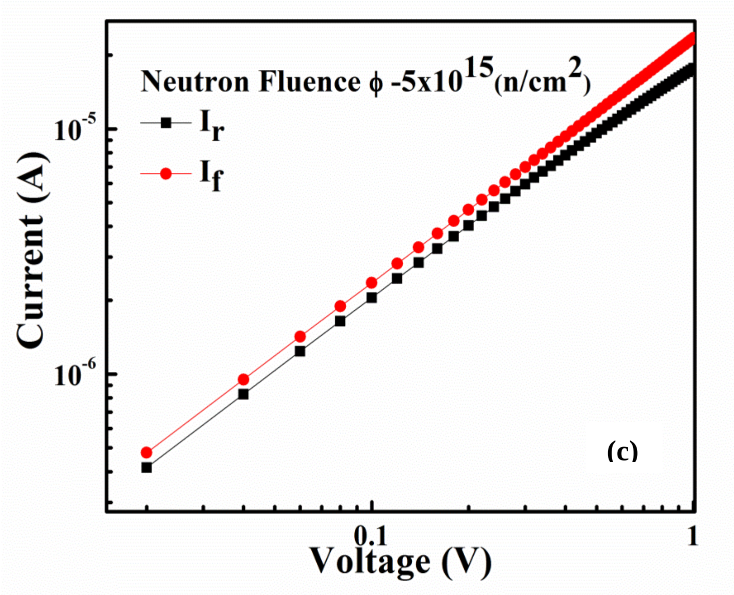

Neutron Fluence ϕ -5x10^15(n/cm^2)
I_r
I_f
Current (A)
10^-5
10^-6
0.1
1
Voltage (V)
(c)

Figure 12

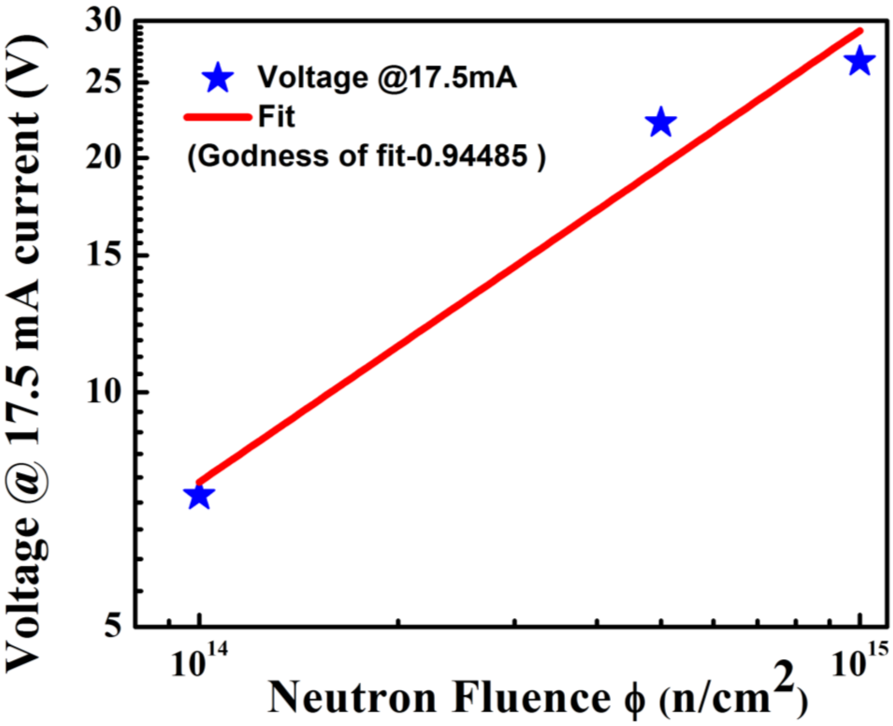
Voltage @17.5mA
Fit
(Godness of fit-0.94485)
Voltage @ 17.5 mA current (V)
30
25
20
15
10
5
10^{14}
10^{15}
Neutron Fluence ϕ (n/cm^2)

Figure 13

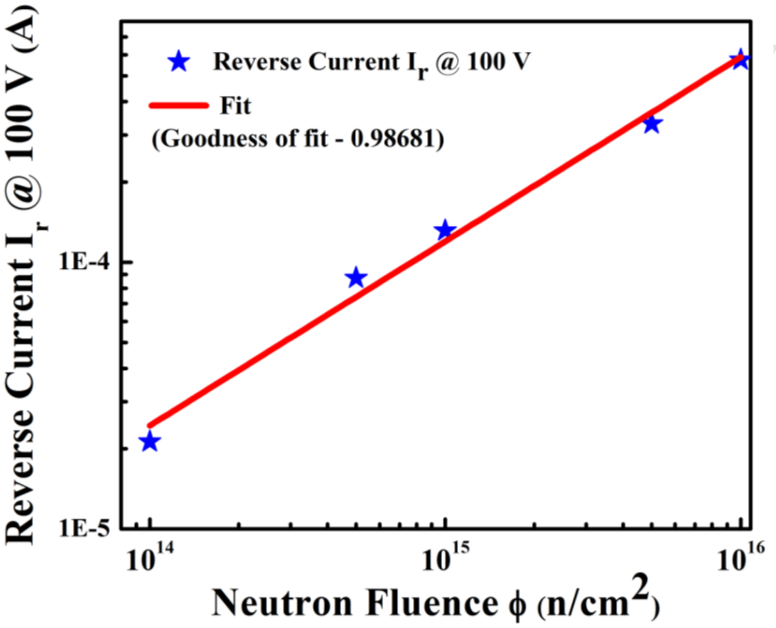
Reverse Current I_r @ 100 V
Fit
(Goodness of fit - 0.98681)
1E-4
1E-5
10^{14}
10^{15}
10^{16}
Neutron Fluence ϕ (n/cm^2)
Reverse Current I_r @ 100 V (A)

Figure 14

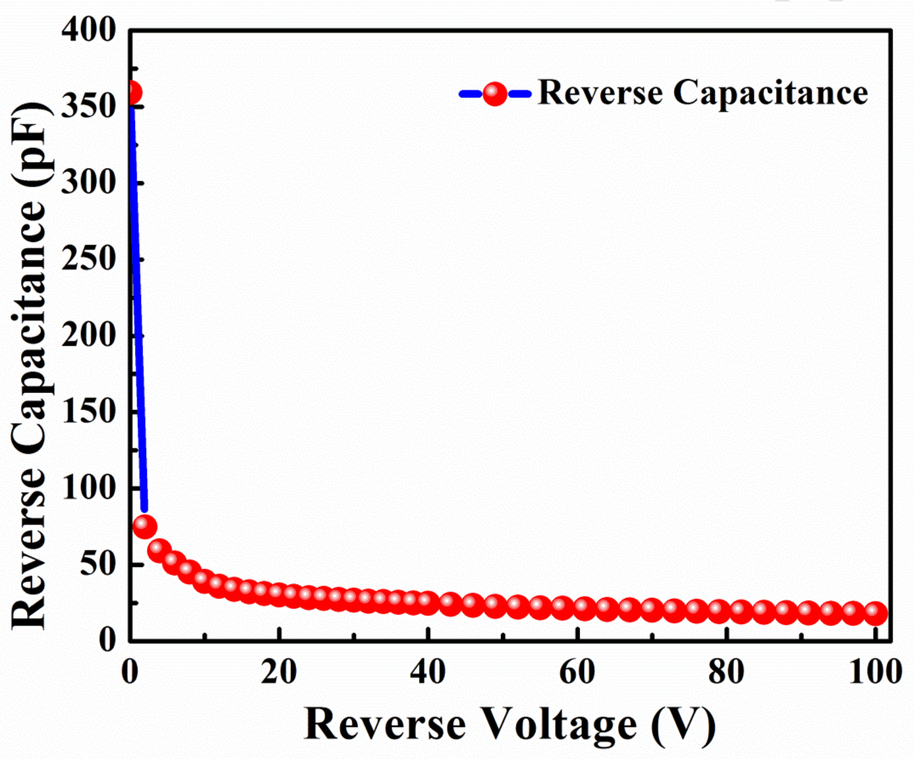
Reverse Capacitance
Reverse Capacitance (pF)
Reverse Voltage (V)
0
50
100
150
200
250
300
350
400
0
20
40
60
80
100

Figure 15

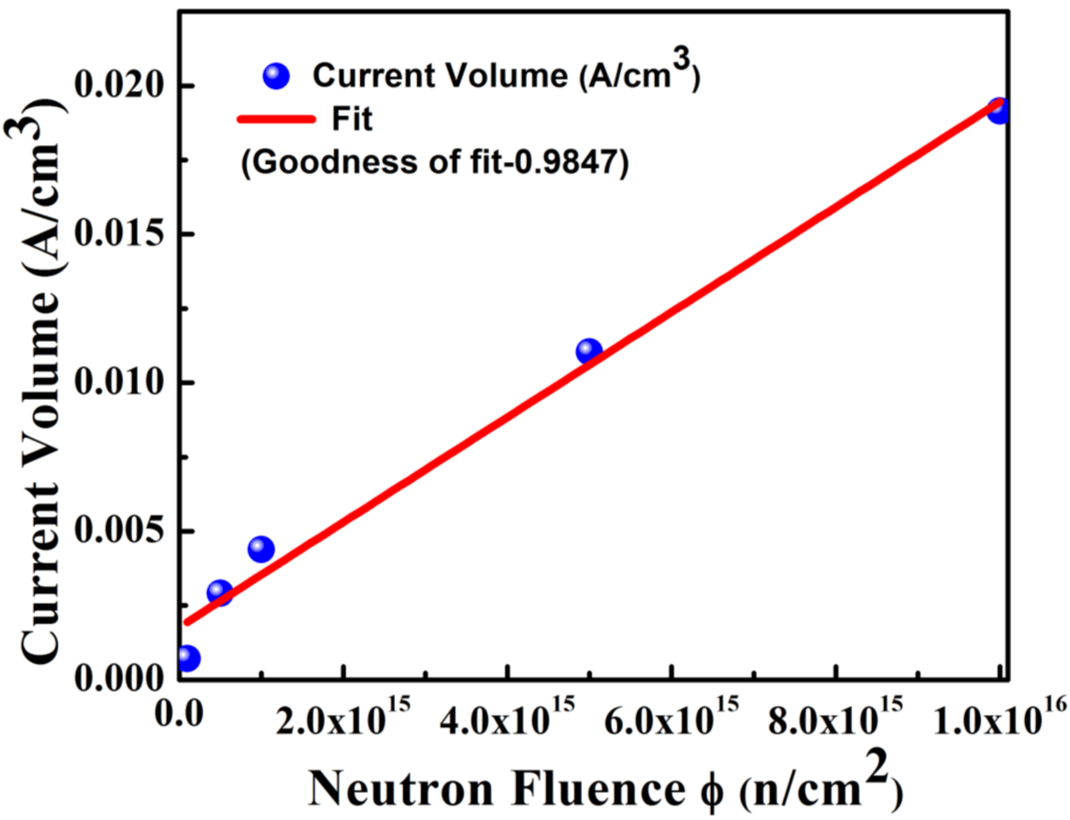
Current Volume (A/cm^3)
Fit
(Goodness of fit-0.9847)
0.020
0.015
0.010
0.005
0.000
Current Volume (A/cm^3)
0.0
2.0x10^{15}
4.0x10^{15}
6.0x10^{15}
8.0x10^{15}
1.0x10^{16}
Neutron Fluence ϕ (n/cm^2)

Figure 16

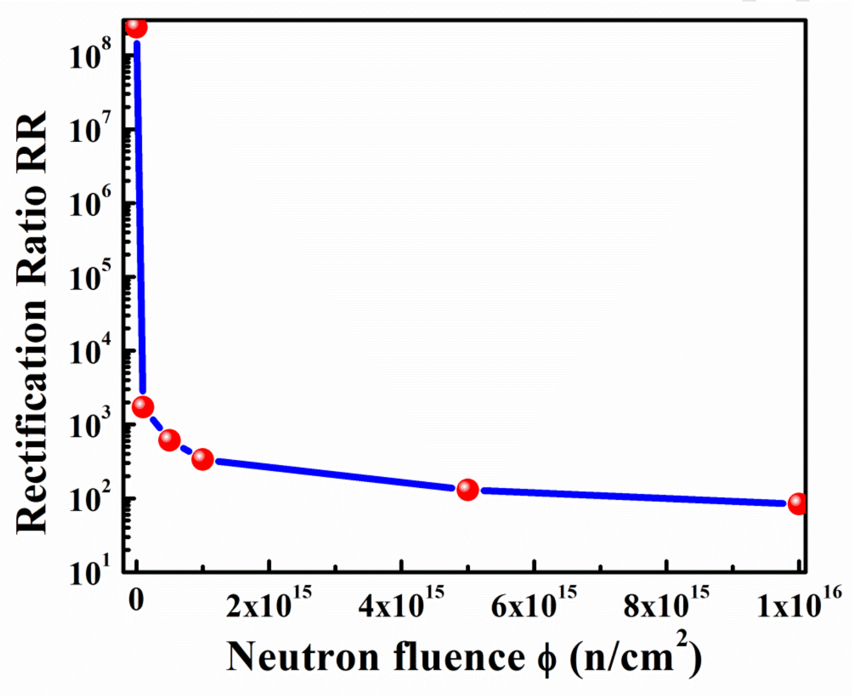
Rectification Ratio RR
10^8
10^7
10^6
10^5
10^4
10^3
10^2
10^1
0
$2x10^{15}$
$4x10^{15}$
$6x10^{15}$
$8x10^{15}$
$1x10^{16}$
Neutron fluence ϕ (n/cm^2)

Figure 17

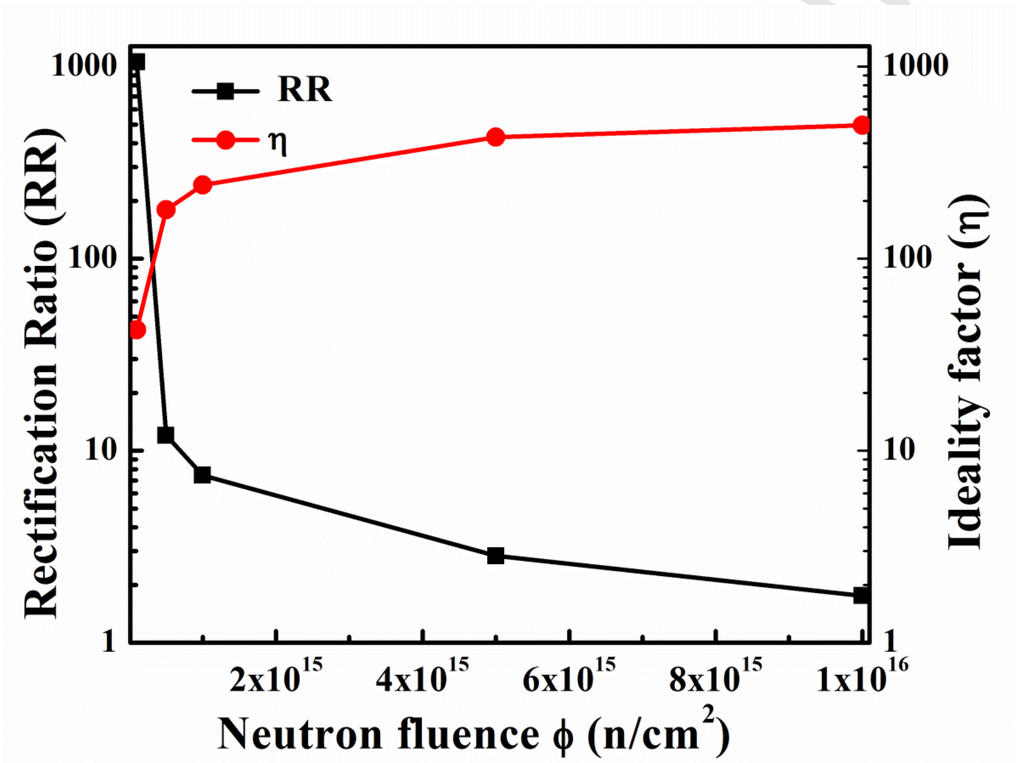
RR
η
Rectification Ratio (RR)
Ideality factor (η)
1000
100
10
1
1000
100
10
1
2x10^15
4x10^15
6x10^15
8x10^15
1x10^16
Neutron fluence ϕ (n/cm^2)